A Small Tokamak "NOVA II"

By

Masayuki FUKAO,* Yuji FUJIWARA,* Hideki ZUSHI,*
Hidetoshi SUEMITSU,** Yasushi TERUMICHI†
and Hiroshi NISHIHARA*

(Received May 27, 1977)

Abstract

A small tokamak, NOVA II, has been designed and constructed. The major radius is 30 cm, the minor radius 6 cm and the maximum toroidal field 15 kG. The device has a removable shell assembly for studying the stablilizing effect of a conductive shell. The basic concept of design and the specifications of the principal components are described. In preliminary experiments, stable discharge was maintained for 15 msec or longer. The electron temperatures measured by diamagnetism and conductivity are both above 100 eV. An electron density of $1-2\times10^{13}\,\mathrm{cm}^{-3}$ was observed by a 6 mm microwave interferometer. Spectroscopy of impurity lines and intensity measurement of hard X-ray radiation are also described.

§ 1. Introduction

The machine "NOVA II" is a small tokamak device whose major and minor radii are 30 and 6 cm, respectively. The maximum intensity of the toroidal magnetic field is 15 kG. The highest vacuum attained is about 3×10^{-8} torr.

The machine has been designed and constructed for the following research programs[1] :

1) Positional stabilization of a plasma in a shell-less tokamak through the program med- and feedback-control of the vertical magnetic field.
2) Effects of conductive and resistive shells on the stabilization of tokamak plasmas.
3) Control of the profile of plasma current by a high frequency field near the lower hybrid resonance.
4) Effects of operating conditions in the earliest stage of discharge on the final equilibrium of the tokamak plasma.

* Dept. of Nuclear Engineering.
** Dept. of Engineering Science.
† Dept. of Physics, Faculty of Science.

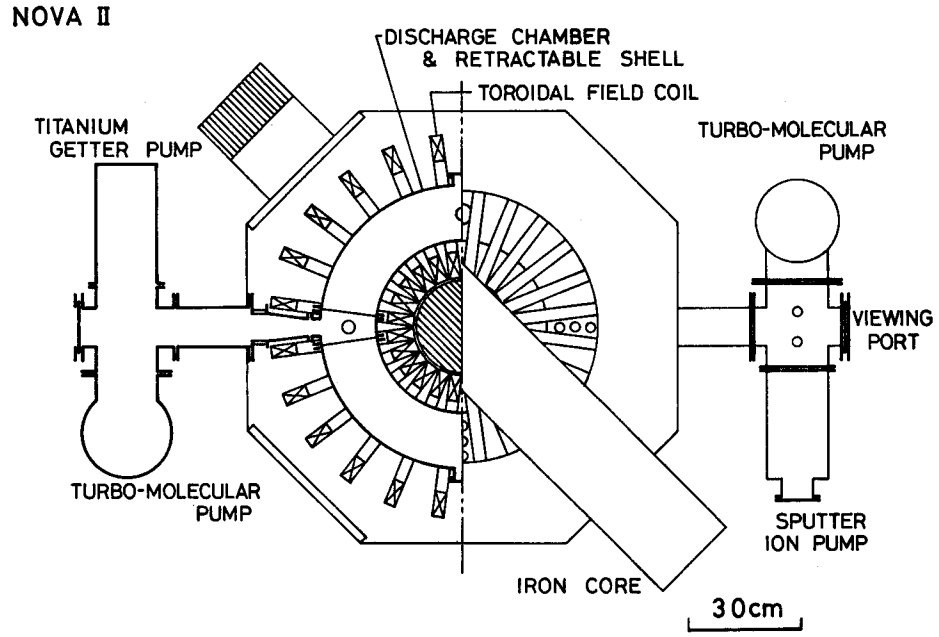

Fig. 1. Schematic drawing of the NOVA II device.

The purpose of this paper is to describe the machine, and to present some of the experimental results obtained during the preliminary operation.

§ 2. Description of Components

The conceptual drawing of the device is as shown in Fig. 1. The geometrical configuration around the plasma column and the position of various windings are shown in Fig. 2 (a) and (b), respecively.

2-1 *Shell*

Thick conductive shells have been used to maintain a stable equilibrium of tokamak plasmas. However, the centering effect of the conductive shell becomes absolutely ineffectual for slow displacements of the plasma column, which may obstruct the very long plasma discharge. Therefore, it is now being planned in many countries to maintain plasma equilibrium by means of an additional vertical field controlled with prescribed programs and negative feedbacks. The shell of NOVA II is removable, so that by observing plasma behaviors with and without the shell, it is possible to investigate the centering effects of the shell and also to try to stabilize the plasma column by an external control field.

The shell is made of aluminum, 1 cm thick. The major radius is 30 cm. The

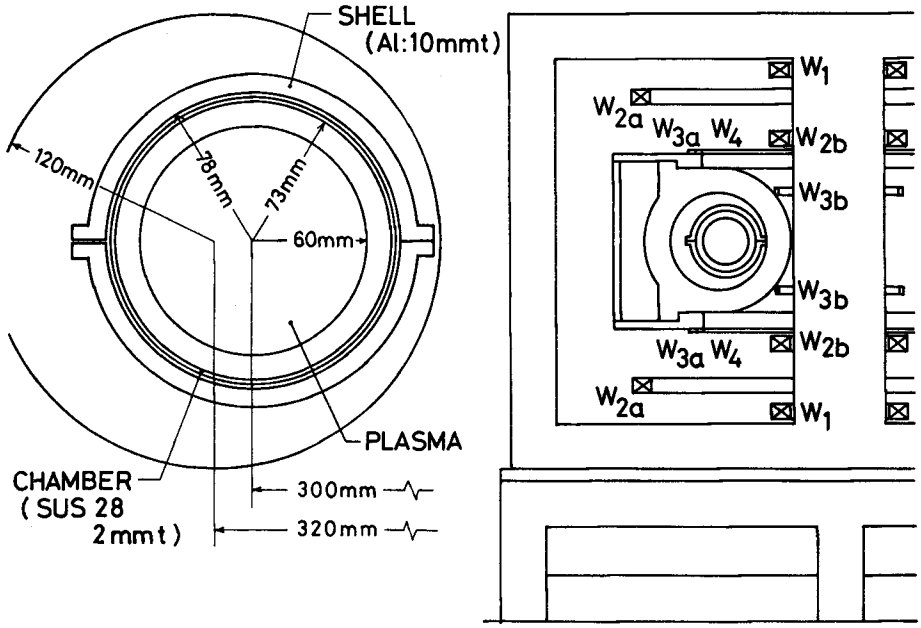

Fig. 2. (a) Geometrical configuration around the plasma.
(b) Location of windings: W_1 ; primary coils of Joule heating, W_2 ; vertical field coils (W_{2a} is also used to be primary coils in a shell-less operation with automatic programmed vertical field), W_3; compensation coils for the vertical comonent of stray field from toroidal colis, W_4; compensation coils for the horizontal components.

inner radius of the transverse cross section is 7.8 cm. It has to have toroidal gaps so that an electric field can be applied to generate the plasma current. Poloidal slits are also necessary to apply the toroidal magnetic field. The shell is made out of two electrically insulated segments separated by the toroidal gaps, being about 12 cm wide, while the outer wall of each segment has a poloidal gap of 1 mm width. Without the gaps, the time constant is estimated at about 18 msec, but the actual time constant with wide gaps should be considerably shorter.

2-2 *Vacuum system*

The vacuum vessel (discharge chamber) is 30 cm in its major radius and 7.3 cm in its inner minor radius. It is made of stainless steel, 2 mm thick. There is no liner that has been equipped in standard tokamaks. Sixteen experimental ports, two evacuating ports and a pair of observation windows are prepared. The vessel consists of four segments which are sealed by Viton O-rings and electrically insulated by teflon sheets. A molybdenum limiter, 0.5 mm thick, is attached to one of the

four joints between adjacent segments. The radius of the limiter aperture is 6 cm.

In order to attain an oil-free high vacuum, the discharge chamber is evacuated by two main turbo-molecular pumps having a capacity 250 liters per second with the aid of an auxiliary pump system having an ion pump and a titanium getter pump. In baking the discharge chamber, the insulated joints are short circuited before the primary windings of the Joule transformer is directly connected to the commercial a. c. power supply of 60 Hz. The shell is insulated thermally and electrically from the chamber by asbesto sheets. A power consumption of 800 W was sufficient to raise the chamber up to 150°C, which is the maximum permissible temperature of a Viton O-ring. The highest vacuum attained by this pump system is 3×10^{-8} torr.

2-3 *Joule heating*

The standard transformer with a circular central leg and two rectangular side legs is made of oriented silicon steel lamination, 0.35 mm thick. The magnetic capacity is about 0.1 V·s. The corners of the core are laminately jointed, and four of them are insulated electrically on the outside by thin plasttic films in order to decouple the core from the toroidal magnetic field system. Observation of the B-H hysterisis characteristic shows that the insertion of an insulator has not brought about an appreciable increase of magnetic reluctance owing to the large joint surface. The bias field to increase the available flux swing is unnecessary, if the core has been sufficiently saturated to negative magnetization before every discharge. Primary windings having a total of 40 turns are located so that the leakage flux at the plasma column is minimized.

The plasma current magnetizes the core in the direction opposite to the magnetization due to the primary current. This is because the plasma column is the secondary circuit of the transformer. The leakage flux due to the secondary magnetization of the core gives rise to a magnetic force which attracts the plasma column toward the central leg of the transformer core. The effect of this magnetic attraction on the plasma equilibrium will be studied in § 2-5.

2-4 *Toroidal magnetic field*

The maximum intensity of the toroidal magnetic field is 15 kG. The winding to generate the toroidal field of this intensity is divided into 24 coil units which have a pancake shape. The unit coils have a winding of 20 turns. The major radius of centers is 32 cm. The bore radius of unit coils is 12 cm. The total inductance in the toroidal and the total resistance are 9.7 mH and 0.112 Ω at 20°C, respectively. The magnetic force toward the axis of torus and the tensile force in the horizontal

median plane are calculated to be 2.1 and 1.6 tons, respectively, per unit coil at the toroidal field of 15 kG.

In order to compensate any stray magnetic field due to the wiring among the coil units as well as irregularities in the arrangement of coil units, the toroidal field coil current is branched into vertical and horizontal compensation coils which consist of pairs of one-turn coil. The compensation coils are located as shown in Fig. 2 (b). For branching the current, shunts of nicrom strip are used.

2-5 *Vertical magnetic field*

The vertical magnetic field was designed to meet the following requirements.

1) The equilibrium condition for a shell-less tokamak plasma derived by Mukhovatov and Shafranov[2] is satisfied. The condition is

$$B_v=\frac{\mu_0 I_p}{4\pi R}\left(1n\frac{8R}{a}+\beta_p+\frac{1_i-3}{2}\right), \qquad \cdots\cdots\cdots(1)$$

where I_p is the plasma current, β_p is the ratio of the plasma pressure to the poloidal magnetic pressure or $2\mu_0\bar{p}/B_p^2$, R is the major radius, a is the minor radius and $\mu_0 1_i/4\pi$ is the internal inductance per unit length of the plasma column. In the first approximation, the intensity B_v required by this equilibrium condition is proportional to the plasma current.

2) The vertical field B_v has a configuration that satisfies the stability condition derived by Osovets[3]

$$\frac{3}{2}>n>0, \qquad n=-\frac{RdB_v}{B_v dR}. \qquad \cdots\cdots\cdots(2)$$

Both of the above conditions must be satisfied in taking account of the attractive force acting between the plasma current ring and the iron core due to the magnetic dipole current in the core induced by the plasma ring current.

Since a calculation of the magnetic field distribution is too complicated to do in the presence of the Joule transformer core, experimental studies of leakage magnetic field were performed using a 1/3 scale model of the core with the windings, in order to determine the optimum configuration of the vertical field coils. The leakage magnetic field, due to the magnetic dipole current in the core induced by the plasma ring current, was experimentally determined by measuring the field in the presence of the core and that in the absence of the core and then subtracting the latter from the former.

Numerical analysis was performed under the following assumptions; (1) the core has a circular cross section of radius d and is infinitely long, (2) permeability of the core is infinitely large, (3) the plasma current I_p flows along a circle being

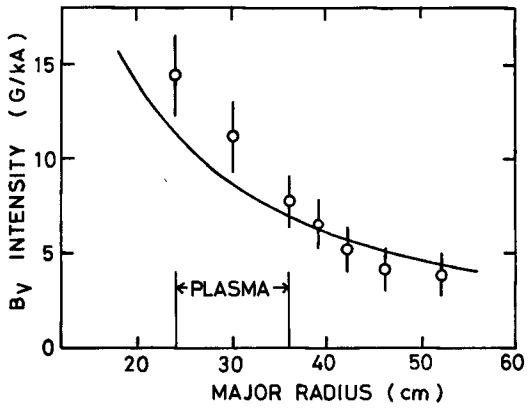

Fig. 3. Vertical field arizing from the magnetic dipole current in the core. Solid line is the calculated value by eq. (3).

coaxial with the cylindrical core. The leakage field, perpendicular to the median plane due to the magnetization of the core, is then expressed in the analytic form as follows[2]:

$$B_z(r, z) = -\frac{\mu_0 I_p}{\pi R}\left(\frac{R}{b}\right)^2 \int_0^\infty \frac{I_0(k)}{K_0(k)} K_1\left(\frac{kR}{b}\right) K_0\left(\frac{kr}{b}\right) \cos\left(\frac{kz}{b}\right) kdk, \quad R > b. \cdots (3)$$

In Fig. 3, the experimental results are compared with the calculation by the above expression eq. (3) for B_v in the median plane, assuming a typical operational condition for the ratio I_p/R of NOVA II. A good agreement is observed in this figure between the theory and the experiment. The field intensity is about $8\,G/kA$. It should be noted that the leakage field attracts the plasma current toward the core center, and that the Osovets condition applies to the distribution of this vertical field.

The outside windings of these vertical field coils are also designed to be able to serve as primary winding of the Joule transformer with the aim that the vertical field produced directly by the primary winding current is proportional to the plasma current I_p. This is because the magnetizing current of the core is so small that the primary current is proportional to the plasma current with a good accuracy. In a shell-less operation, therefore, the vertical field serves to be automatically programmed in the first approximation.

2-6 *Power supplies*

The major components of the power supply system are listed in Table I. The circuit diagram and the operation time sequence are as shown in Fig. 4.

A magnetically driven vacuum sealed metal contact is used as the main switch

Table I Specifications of the power supplies.

	Toroidal field	Joule heating	Vertical field
Capacitance	12 mF	a: 200 μF b: 12 mF	a: 200 μF b: 800 μF
Maximum charging voltage	5 kV	a: 5 kV b: 0.5 kV	a: 5 kV b: 1 kV
Maximum stored energy	150 kJ	3.4 kJ	2.85 kJ
Rise time	17 ms (1/4 period)	variable	variable
Switching	Vacuum sealed metal contact	Ignitron	Ignitron
Crowbaring	Diodes	Diodes	Diodes

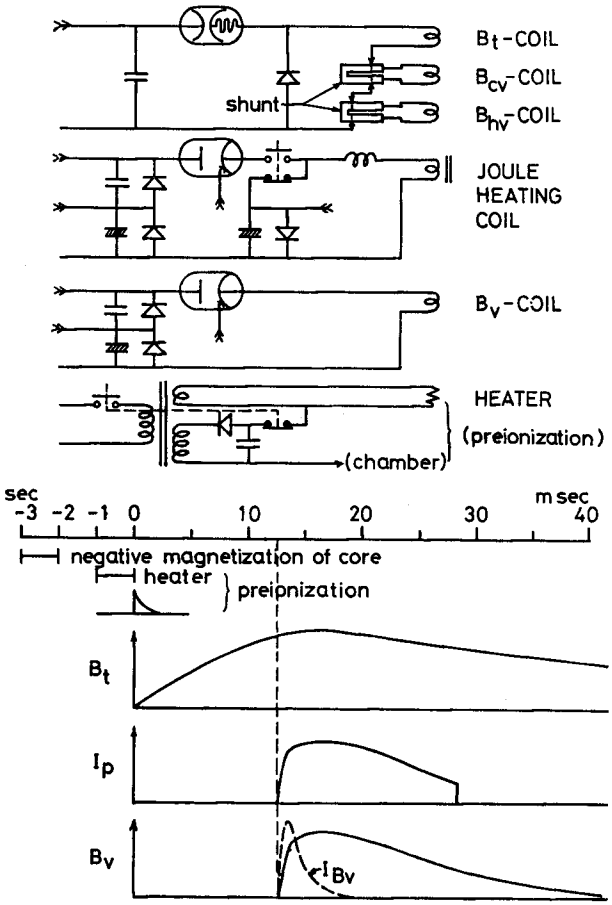

Fig. 4. Circuit diagram and operation time sequence of the NOVA II, I_{Bv} shows the current flowing in the vertical coil in the presence of a conductive shell.

of the toroidal field circuit. Though the magnetic switch has an appreciable time jitter, the effect is nullified by triggering the pulse train generator, which controls the trigger times of other circuits, through the terminal voltage of the toroidal field coils. The branching ratio of the current into the compensation coils is adjusted by sliding a pair of contacts on a shunt resistor made of nicrom strip, 20 mm wide and 1.7 mm thick. The time constant of the compensation coils and series resistors should be short enough so that the branched current may be proportional to the main coil current.

The power supply for Joule heating consists of a high voltage small capacitance condenser bank and a large capacitance low voltage bank. During the earliest period of the plasma current build-up, where a strong toroidal electric field is necessary, the high voltage bank supplies the required high primary voltage, while the large capacitance bank takes over the duty of keeping the plasma current almost constant during a long period of plasma discharge. The primary voltage waveform from both banks is smoothly connected through diodes. The negative power supply is used to eliminate the residual magnetization of the core and swing it into the negative saturation level, so that the available flux swing is maximized. An external inductance is connected in series between the power supply and the primary winding in order to externally control the rise time of the plasma current by varying the value of inductance and also to reduce the effects of miscellaneous intrinsic origins in the plasma to the current growth rate. This control is promising for the study of phenomena, such as the formation of runaway electrons and the desorption of impurity atoms from the wall, occurring in the early stage of the current build-up, when a high toroidal electric field exists and is apt to cause large fluctuations of plasma.

The power supply for the vertical field also has a structure similar to that for the Joule heating circuit. In operations with the conductive shell, a short and intense current pulse is applied to the vertical field coils so that the effective vertical field applied to the plasma column inside the shell satisfies the plasma equilibrium condition.

Pre-ionization is performed by applying a high voltage pulse between the vacuum chamber and the hot tungsten filament, inserted immediately behind the limiter aperture, at the instant when the toroidal magnetic field starts to rise.

§3 Characteristics of Plasma in NOVA II

3-1 *General discharge characteristics*

Typical operational conditions during the preliminary experiments are as follows:

Gas: Hydrogen of filling pressure 2.2×10^{-4} torr.

Toroidal magnetic field: 9 kG.

Conductive shell: Mounted.

Figure 5 shows typical waveforms of the plasma current, the one-turn loop voltage together with the intensities of X-ray radiation, H_β and OIII spectral lines. The duration of stable discharge was 15 msec or longer and the maximum plasma current was about 10 kA.

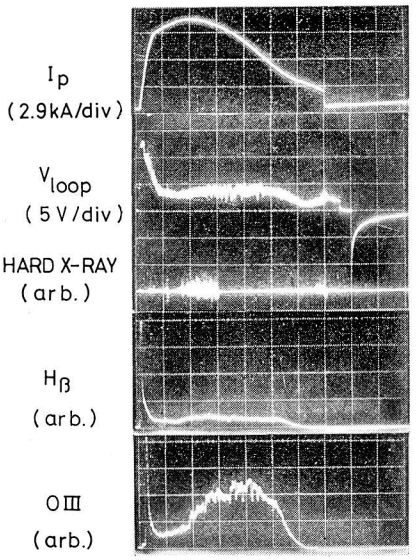

Fig. 5. Typical waveforms of the NOVA II. From the top to the bottom traces plasma current, one-turn loop voltage, hard X-ray, H_β (4961A) and O III (3265A) spectral lines. Conditions; B_t=8 kG and p_f=2.2 10^{-4} torr H_2.

In an early series of experiments, a train of negative spikes was observed in the one-turn loop voltage but it disappeared after adjusting the operational conditions as described below. As for the compensations for the stray fields, both the vertical and horizontal components from the toroidal field coils are very effective. Under imperfect compensation, the discharge period is shortened and the lower limit of operating gas pressure for ignition is highly raised. An externally applied vertical field is essential in order to ensure long stable discharges. It was observed that the X-ray radiation was intensified with a decreased initial gas pressure. This may be attributable to the fact that the number of runaway electrons increases remarkably at lower gas pressures. Upon increasing the safety factor by intensifying the toroidal magnetic field, the MHD instabilities are suppressed considerablly, resulting in a much smoother waveform of the one-turn loop voltage. Discharge characteristics are also strongly dependent on the number of shots for discharge cleaning. The reproducible discharge characteristics described above are observed after about two hundred shots for discharge cleaning.

3-2 *Electron density*

Figure 6 shows time behaviors of the averaged electron density for three different values of the filling gas pressure 1.3, 2.2 and 3.3×10^{-4} torr under the typical operating condition previously described. The electron density was measured by a 6 mm microwave interferometer of the fringe-shift type. The averaged density obtained by this method is given by

$$\langle n_e \rangle = \frac{1}{a}\int_0^a n_e(r)\, dr, \qquad \cdots\cdots\cdots(4)$$

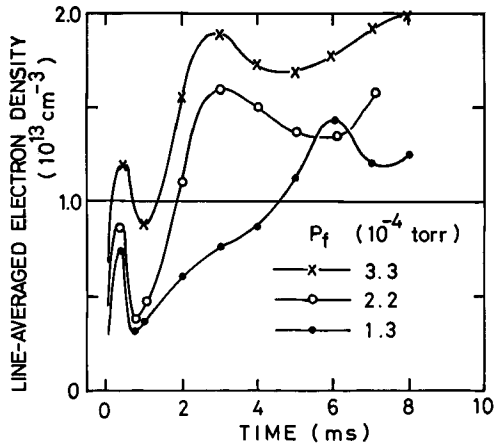

Fig. 6. Line-averaged electron densities measured by a 6 mm microwave interferometer.

assuming that the microwave beam is sufficiently thin and suffers no diffraction. It is observed, as shown in Fig. 5, that the averaged density $\langle n_e \rangle$ reaches its first maximum at about 0.5 msec after ignition. A rapid fall follows the peak, and then the density rises again until it reaches the second maximum, which is about 1.5×10^{13} cm^{-3} for the initial pressure of 2.2×10^{-4} torr.

The averaged value defined by eq. (4) depends upon the profile of the density distribution $n_e(r)$. In a case where the profile is convex and represented by

$$n_e(r)=n_0\left(1-\frac{r^2}{a^2}\right), \qquad \cdots\cdots\cdots(5)$$

the averaged $\langle n_e \rangle$ is $(2/3)n_0$, while the average over the cross section of the plasma column, $\bar{n}_e$, is given by

$$\bar{n}_e=n_0/2 \qquad \cdots\cdots\cdots(6)$$

In the case of the concave profile expressed as

$$n_e(r)=n_0(r/a)^2, \qquad \cdots\cdots\cdots(7)$$

the average n_e is reduced to $n_0/3$, although the cross sectional average remains the same as above, i. e. $\bar{n}_e=n_0/2$. Therefore, the rapid fall observed in the electron density may be, at least partly, attributable to the hollowing of the distribution. In fact, hollow electron density distributions have been observed in T—6 plasma, at an early stage of discharge, by using a multichannel microwave interferometer[4]. The hollowing of the density distribution will be discussed again in connection with the measurement of plasma temperature through diamagnetic flux.

3-3 *Diamagnetism and conductivity temperature*

Measurement of the diamagnetic effect of the plasma is useful for determining the time development of the transverse plasma energy[5]. The diamagnetic flux $\Delta\Phi$ is given by the well-known expression

$$\Delta\Phi = -\frac{\mu_0^2 I_p^2}{8\pi B_t}(1-\beta_p), \qquad \cdots\cdots(8)$$

where

$$\beta_p = \bar{p}/(B_p^2/2\mu_0), \qquad \cdots\cdots(9)$$

and $\bar{p}$ is the transverse kinetic pressure averaged over the plasma column cross section, which is $\overline{n_e T_e + n_i T_i}$.

The diamagnetic flux was detected by means of two differential poloidal loops mounted in a toroidal shell gap. Loop A is wound in the surface of the discharge chamber, while loop B is stuck on the inner surface of the toroidal magnetic field coil. Since the power supply for the toroidal magnetic field has a very low internal impedance, the magnetic flux through loop B is not changed appreciably by the presence of the diamagnetic current in plasma. On the contrary, the magnetic flux through loop A is slightly changed by the diamagneic effect of the plasma. The two loops are connected reversely and adjusted so that the electric motive forces induced by the fluxes just cancel out each other in the absence of the plasma. The signal due to the diamagnetic flux in the presence of the plasma is fed to an integrator and it immediately yields the diamagnetic flux.

The poloidal beta β_p determined from the plasma diamagnetism is shown in Fig. 7 as a function of the time after ignition. This figure also presents the ratio $\overline{n_e T_e + n_i T_i}$ to the averaged electron density $\langle n_e \rangle$, which may be referred to as a plasma temperature. As mentioned in § 3-2. the averaged density $\langle n_e \rangle$ is suspected

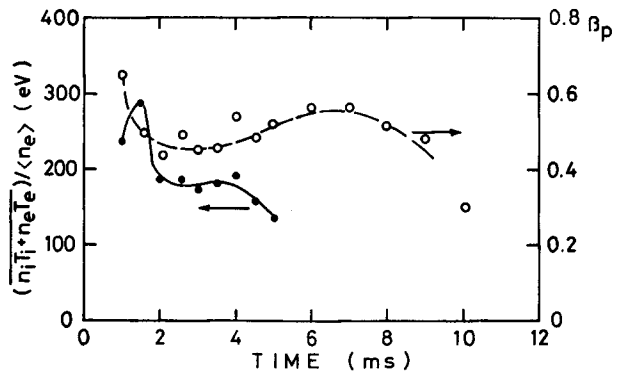

Fig. 7. Transverse plasma temperature and β_p measured through diamagnetism.

to be underestimated in the early stage of plasma discharge. The peak which appears in the waveform of the plasma temperature of Fig. 7, at around 1 msec, may be attributed to this underestimation. Therefore, the peak may be eliminated by correcting the density of electrons.

The plasma temperature determined at the flat top of the plasma current is about 180 eV, as shown in Fig. 7. The electron temperature can also be determined from the electric conductivity measurement.[6] Assuming that there is no appreciable change in the internal inductance of the plasma column, a resistivity of 0.18×10^{-3} Ω-cm was experimentally obtained at the plasma current maximum. This value of resistivity yields an electron temperature of 57 eV, if the effective ionic charge is unity. The ion temperature T_i is estimated to be appreciably lower than the electron temperature T_e, taking into account the energy containment time and the energy relaxation time between electrons and ions through the Coulomb collision. This large discrepancy between the diamagnetic-temperature and the conductivity-temperature may be partly due to the impurities of higher Z-values. Assuming that the effective value Z_{eff} is four, the conductivity temperature is estimated to be 118 eV. There are some ambiguities in the measurement of the diamagnetism, i. e. the effects of the presence of the conductive shell and the vacuum chamber, and also the flux conservation inside loop B. The former effect is, at least partly, diminished by the process of cancelling out the 0-th order toroidal field between loops A and B, in which the signal of loop B partially bypassed the integrator and was added to its output in order to eliminate the effect[7]. The flux conservation could be analytically estimated, assuming that the current distribution in toroidal field coils is axially symmetric around the major axis. The real current distribution, lumped in pancake-shaped coil units, brings about some error in the flux conservation inside loop B located between the adjacent coil units. These effects described above are estimated to yield some ten per cent of error in measuring the diamagnetic flux.

3-4 *Impurity line spectroscopy*

Impurity lines between 2300 and 8000 A were observed, using a grating spectrometer with a collimator focal length of 50 cm. Both the observation window and the lens are made of quartz glass. The following impurity lines have been identified by a spectrograph analysis:

Oxygen; OII, OIII, OIV, OV, OVI.

Carbon; CII, CIII, CIV, CV.

Molybdenum; MoI, MoII.

Fluorine; FII, FIII.

Figure 8 shows the experimentally observed line intensities for oxygen as func-

tions of time. The observed lines and the related potentials are listed in Table II. The radiation from the impurity species appears in the early stage of discharge, where the electron temperature grows monotonously with time. The time behaviors of the electron temperature which fit the observed time histories of line intensities are now being investigated[8].

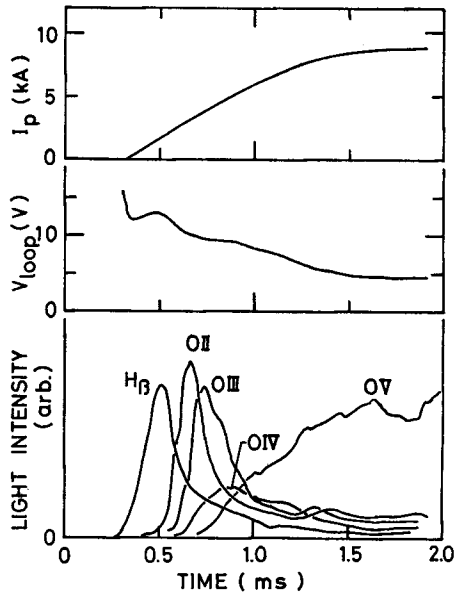

Fig. 9. Time histories of hydrogen and oxygen spectral lines in an early stage of discharge. The observed lines and the related potentials are listed in Table II.

3-5 *Hard X-ray measurement*

An NaI (Tl) scintillation detector was used in measuring the hard X-ray emitted as Bremsstrahlung when run-away electrons impinge on the surface of a limiter plate. From the measurement of the spatial distribution, the X-ray source is concentrated upon the limiter. Under a typical operational condition of NOVA II, the hard *X*-ray radiation starts at 0.6 to 0.7 msec after ignition when a large amount of runaway electrons is produced as a result of the sudden decrease in the electron population near the plasma axis by hollowing the density profile as described in § 3-2. The radiation disappears for a while in the middle part of the discharge period, because the production of runaway electrons is impeded by an increased plasma density through the incidence of neutral particles and impurities. The hard X-ray radiation appears again in the last stage of discharge. It has been observed that the radiation is always coincident with a smooth part in the oscillogram of the one-turn loop voltage. In other words, the disappearance of radiation is always accompanied by large fluctuations in the loop voltage, as shown in Fig. 5. The production of run-

Table II Observed spectral lines and the related potentials.

Line	Wave length	Ionization potential	Excitation potential
H_β	4861.3 A	13.6 eV	12.6 eV
O II	4414.9	35.1	26.3
O III	3265.5	54.9	40.3
O IV	3071.7	77.4	48.4
O V	2781.0	113.9	72.3

away electrons depends strongly upon the plasma density, i. e. upon the filling gas pressure.

§4 Summary

The results of the present study are summerized as follows.

1) A stable plasma with a discharge time of 15 msec has been realized in a small tokamak device NOVA II under the operational conditions that the toroidal field is 9 kG, the maximum plasma current is 10 kA and the one-turn loop voltage is 3 V.
2) The electron temperature determined from the electric conductivity is 57 eV when the effective ionic charge is assumed to be unity.
3) The plasma temperature determined from the diamagnetism measurement is about 180 eV.
4) The electron density is about $1.5\times10^{13}\mathrm{cm}^{-3}$ for the initial filling gas pressure of 2.2×10^{-4} torr.
5) In the early stage of discharge, it seems that there occurs either a sudden decrease of electron population or a hollowing of the electron density distribution.

The experimental results described above have been obtained with the condutive shell mounted. Almost the same results have been obtained without the shell, when a vertical field coil was used as the primary winding of the Joule transformer, although larger fluctuations appear in the one-turn loop voltage than in the case with the conductive shell. A description about the characteristic without the conductive shell is being prepared for another report.

Acknowledgment

The authors are most grateful to Drs. H. Momota, H. Kubo, S. Nakamura, T. Yuyama and H. Oshiyama for their encouragement and valuable discussions in planning this research and constructing the device. They also would like to thank Drs. S. Itoh, S. Fujiwaka and M. Ooi for useful suggestions about designing the device, and Y. Shimidzu for the construction of power supplies and electronic instruments. This work was supported by Grant-in-Aid for Scientific Research from the Ministry of Education.

References

1) The NOVA Group; MEMOIRS of the FACULTY of ENGINEERING, KYOTO UNIVERSITY **35**, 297 (1973)
2) V. S. Mukhovatov and V. D. Shafranov; Nuclear Fusion, **11**, 605 (1971)
3) S. M. Osovets; "Plasma Physics and the Problem of Controlled Thermonuclear Reaction" **2**,

322 Pergamon Press (1959)
4) V. S. Vlasenkov, V. M. Leonov, V. G. Merezhkin and V. S. Mukhovatov; Nuclear Fusion **13**, 509 (1973)
5) S. V. Mirnov; Matt-Trans-87 (1967)
6) L. Spitzer; "Physics of Fully Ionized Gases" Interscience Publisher, New York (1962)
7) M. A. Rothman; Plasma Physics **10**, 86 (1968)
8) L. M. Goldman and R. W. Kilb; Plasma Physics **6**, 217 (1964)